Int. J. Electrochem. Sci., 9 **(2014)** 5850 - 5863

International Journal of
ELECTROCHEMICAL
SCIENCE
www.electrochemsci.org

Corrosion Resistance of 5052 Al-alloy with a Zirconia-Rich Conversion Coating Used in Bipolar Plates in PEMFCs

Te-Yuan Chiang[1], *Ay-Su*[1,*], *Lin-Chang Tsai*[2], *Hung-Hua Sheu*[3,*], *Chen-En Lu*[3]

[1] Department of Mechanical Engineering, Yuan-Ze University, Taiwan, ROC
[2] Department of Mechatronic, Energy, and Aerospace Engineering, Chung Cheng Institute ofTechnology, National Defense University, Taiwan, ROC
[3] Department of Chemistry & Materials Science Engineering, Chung Cheng Institute of Technology, National Defense University,Taiwan 335, ROC
[*]E-mail: meaysu@saturn.yzu.edu.tw; HHSHEU@ndu.edu.tw

Received: 21 July 2014 / *Accepted:* 18 August 2014 / *Published:* 25 August 2014

In this work, a Zr-Cr oxide conversion coating was formed by a conversion process to improve the corrosion resistance of 5052 aluminum alloy BBPs. The main contents of the conversion coating included Zr, Cr and Si oxide, and the thickness of conversion coating was approximately 100 nm. The thin conversion coating exhibited the conductivity of the aluminum alloy substrate. The experimental results herein indicate that the optimal operating parameter (I_{corr}) of the conversion coating was reached at 5 min (cracks-less) of conversion, with a value of about 9.302×10^{-8} A/dm^2 at 25℃ and 5.760×10^{-8} A/dm^2 at 80℃, respectively. The potentiostatic polarization curves of the coating following 5 min of conversion demonstrate that the coating did not exhibit pitting corrosion. An SEM micrograph confirms that the surface of conversion coating was free of pitting corrosion. ICP analysis also reveals that the amount of aluminum that was dissolved from substrate when the coating was formed by 5 min of conversion was very low. In single cell testing, the initial aluminum substrate yielded a high current density of approximately 1300 mA/cm^2 at the beginning of the test, dropping to 80 mA/cm^2 after working for 100 h. The substrates with conversion coatings passed a current density of around 1000 mA/cm^2 at the beginning of the test, dropping to 500 mA/cm^2 after 100 h of operation, revealing that the conversion process improves the corrosion resistance of aluminum alloy BBPs.

Keywords: aluminum alloy, BBPs, Zirconia-rich conversion coating, corrosion, PEMFCs, single cell,

1. INTRODUCTION

Global warming as a result of energy consumption is a serious issue , which has attracted a great deal of attention globally. Therefore, various countries have made great efforts to develop

alternative energies and generation technologies. Fuel cells are one source of alternative energy that is not limited by geographical location or the ecological environment [1-4]. Among diverse fuel cells, proton electrolyte membrane fuel cells (PEMFCs) have several advantages, including small volume, lightness, a high power efficiency and a low operating temperature [5-8]. Graphite is commonly used in bipolar plates, but it represents large percentages of the mass and volume of a PEMFC, and are difficult to transport [9-11]. To improve the weight and volume of PEMFCs, metal is a preferred material for use in the bipolar plate; it is easy to fabricate, has excellent conductivity, and superior mechanical properties, all facilitating the manufacture of a light PEMFC with a small volume [9-13].

Aluminum alloy has several advantages over graphite, including excellent mechanical strength, high plasticity, and low cost. Additionally, the weight of aluminum alloy is only about 65% that of stainless steel [8]. The use of aluminum alloy to reduce the weight of PEMFCs is favored over that of other metals, such as stainless steel (too heavy) [8], titanium alloy (too expensive) [14] and magnesium alloy (low formability) [15]. However, after a long period of operation, the cations in fuel cells, such as SO^{4-}, SO^{3-}, HSO^{4-}, SCO^{3-} and HCO^{3-}, dissolve into water [16-19]; the metallic bipolar plate exhibits electrochemical corrosion and its resistance therefore increases [19-22]. The metallic ions that dissolve from the substrate as a results of electrochemical corrosion cause the catalyst within the MEA to undergo a poisoning reaction, which contaminates the proton exchange membrane and reduces the efficacy of the fuel cell [23]. Therefore, in several countries, extensive efforts have been made to modify the surfaces of metallic bipolar plates by coating them with coatings with a high corrosion resistance [20-22], improving both their corrosion resistance and their conductivity.

In general, aluminum can be oxidized easily in the atmosphere and surface modification is required to improve the corrosion resistance and conductivity of coatings. Common surface modification methods can be classified as dry (PVD, CVD) or wet (electroplating, chemical plating and conversion). Dry methods require expensive equipment to generate a high-vacuum and high-temperature environment, and are not suitable for producing large numbers of bipolar plates. Wet methods have such advantages as requiring simple equipment, being easy to implement and being low-cost. Therefore, the wet methods are suitable for producing large numbers of bipolar plates.

In this study, the 5052 aluminum alloy was used as a substrate. However, the fact that aluminum alloy corrodes easily in acidic solution [23-24] presents a challenge to the modification of its surface. Typically, the surface of aluminum alloy can form a thin and dense aluminum oxide layer that has excellent corrosion resistance but low conductivity and this aluminum oxide layer inhibits the effective operation of the bipolar plate in a PEMFC. The conversion process [25-29] can yield a thin conversion coating that has excellent corrosion resistance and conductivity. The process is favored because it requires simple equipment; it simple to implement, and is low-cost [29-33].

Chromate conversion coatings (CCCs) have excellent corrosion resistance and are utilized widely to improve the corrosion resistance and adhesion of various raw materials [34, 35]. Chromate conversion coatings have been developed over a long period; they are useful anodic corrosion inhibitors for zinc, iron and aluminum alloy. However, the conventional Cr(Ⅵ) plating process is highly toxic so alternatives must be found. The European Union passed the WEEE and ROHS directives to restrict the use of Cr(Ⅵ) in electrical and electronic equipment. The U.S. completely

prohibited the use of Cr(Ⅵ) in industry in 2010. Developed countries have made extensive efforts to develop a Cr(Ⅲ) plating process to replace the conventional Cr(Ⅵ) plating process [28-32].

The solution that is added to chromium sulfate, zirconate and fluoroborate, and then used as an electrolyte to form trivalent chromium conversion coating in 5052 aluminum alloy substrate. Some of our earlier investigations [26, 27] investigated the corrosion resistance, microstructure, and growth mechanism of trivalent chromium conversion coatings. The composition of the conversion electrolyte importantly affects the growth and chemical composition of Zr-Cr oxide conversion coating. The literatures [36] demonstrate that the zirconium oxide has some excellent properties, such as high strength, hardness, corrosion resistance and chemical stability and these properties can increase the corrosion resistance of Zr-Cr oxide conversion coatings. In this study, an aluminum alloy substrate, after the conversion process, is used to form a bipolar plate, and the properties of the conversion coating are also analyzed. The efficacy of a single cell is also examined.

2. EXPERIMENTAL

2.1. Materials

The material studied herein is 5052 aluminum alloy. The 5052 aluminum alloy sheet had a thickness of 3 mm. The main alloy elements and their maximum atomic weight percentages were 0.45% Si and Fe, 0.1% Cu, 0.1% Mn, 2.2-2.8% Mg, 0.15% Cr, and 0.1% Zn with the balance aluminum. Test samples were cut into coupons with dimensions of 50mm×50mm×3mm. All chemicals used were of analytical grade and all solutions were prepared using denionized water.

2.2. Surface modification process

The surface of the aluminum alloy plate was rubbed with 2000# abrasive paper; degreased using ethanol for 5min; activated by immersion in 3% aqueous NaOH for 3 min, and immersed in nitric acid (1:1 HNO_3) for 2 min to undergo the chemical conversion treatment. The bath that was used in the chemical conversion treatment contained $KZrF_6$, $Cr(SO_4)_2$, buffer and surfactant. Chemical conversion treatment was carried out at 35℃, for 1, 5 or 10 min. The pH of the conversion bath was adjusted to pH= 3.8 by adding sulfuric acid. When the CCC process was complete, all of the coatings were rinsed in distilled water and dried in air at room temperature for 24 h.

2.3. Measurements and analysis

The surface morphologies of conversion coatings were studied using a field-emission scanning electron microscope (FE-SEM). A transmission electron microscope (TEM) was utilized to examine the cross-sectional microstructure of the conversion coating. The X-ray photoelectron spectrum (XPS) of the conversion coating was measured using an ESCA250 (VG Science Inc., UK) spectrometer with monochromatic Mg K_ radiation. The pressure in the spectrometer was approximately 10^{-9} Torr during

the measurement. The binding energy peaks of the detected photoelectron were referenced to the C 1s peak at 285 eV. Potentiodynamic polarization tests were performed using a three electrode potentiostat system to evaluate the electrochemical behavior of the simply chromized and rolling-chromized steel sheets. A saturated calomel electrode (SCE) was used as a reference to measure the potential across the electrochemical interface. The tests were conducted by sweeping the potential from −0.5V to 0.8V at a scanning rate of $0.5mVs^{-1}$ in a 0.5M H_2SO_4 solution at room temperature, without the purging of any gases. Before the tests were performed, all specimens were degreased and rinsed using deionized water. Each specimen was tested in a fresh corrosion bath.

Techniques for measuring the interfacial contact resistance has been well documented [4-5, 37-39]. In this work, the interfacial contact resistance between the specimens and GDL (carbon paper) was evaluated using method similar to that developed by Wang *et al.* [4-5,39].

Measured cell voltages and power densities as functions of current density in the single cells were plotted as I–V and I–P curves in the operating operational region of 0.9–0.35 V. The long-term performance of each cell was tested at an operating voltage of 0.5V for 100 h. The as-built single cell was operated at 50 ◦C at ambient pressure. Pure hydrogen and air, which were fully humidified at 70 ˚C, were the reactant gases at the anode and cathode sides, respectively. The flow rate of both the anode gas and the cathode gas (QA and QC) was OR controlled at 300 cm^3 min^{-1}. Before the cell was used, it was purged of residual gases using nitrogen.

3. RESULTS AND DISCUSSION

Figure 1 presents the SEM morphologies of specimens underwent conversion for 0, 1, 5 and 10 min, respectively. The surface morphology of the aluminum substrate without chemical conversion process was rough surface and exhibited potholes (Fig. 1(a)). Figure 1(b) shows OR displays the specimen following chemical conversion for 1 min: on the substrate was deposited a very thin oxide layer, owing to the short conversion time, and the deposited layer did not completely cover the substrate. The surface of the specimen exhibited many potholes and particles. After 5 min of conversion, a uniform oxide layer completely covered the substrate without any defects or potholes; the deposited oxide layer was dense. Figure 1(d) presents micro-cracks in the conversion coatings after 10 min of conversion. The micro-cracks probably were formed by the residual stress within coatings on account of the thickness of the layer that resulted from prolonged conversion. The stress is generated by the dehydration, which eliminates the water from the water-rich compounds a phenomenon that increases with the time for which the coatings are exposed to the atmosphere. Therefore, conversion coatings shrink over time, causing them to crack. The various contents of the coatings also generates stress that produces micro-cracks [26-27]. The micro-cracks within the conversion coatings reduce the corrosion resistance and increase the contact resistance of the BBPs, reducing the efficacy of the fuel cells in which they are used.

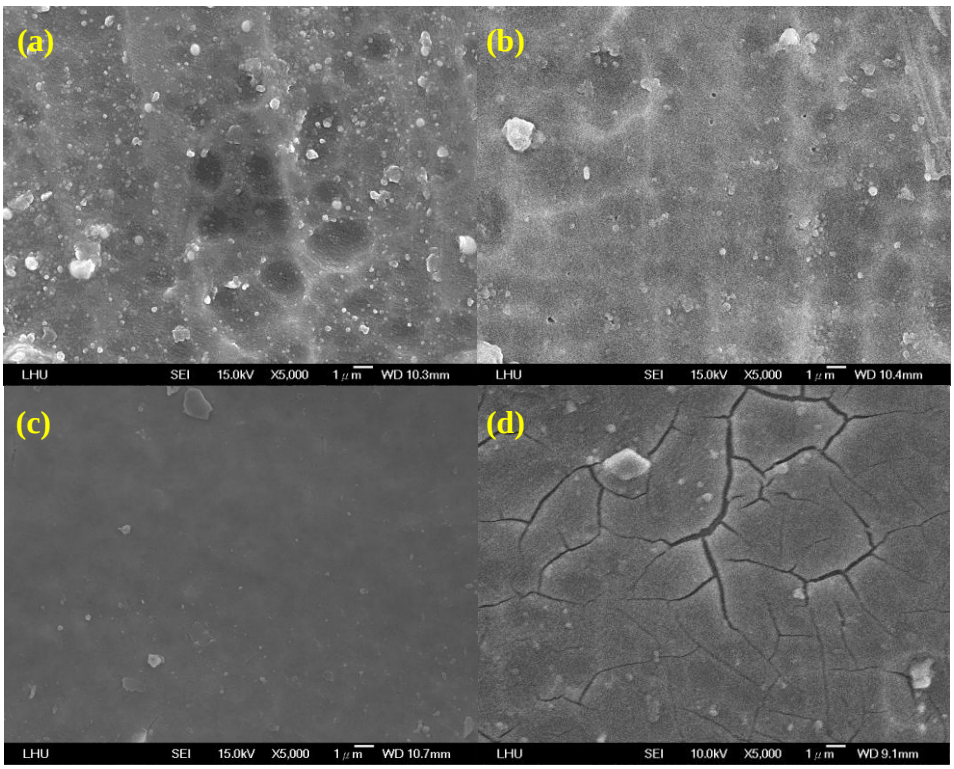

Figure 1.SEM micrographs of chemical conversion coatings on 5052 Al alloys at 35℃ at various chemical conversion treatment times: (a) no treatment, (b) 1min, (c) 5min and (d) 10min.

The ambient temperature of the fuel cell increases as it is operated. Acid radicals are dissolved from the proton exchange layer, chemically reacting with the water to form an acid solution within the flow channels of the BBPs. The above conditions cause high-temperature corrosion behavior in the BBPs, reducing the efficacy of the fuel cell. In this work, high-temperature corrosion of the BBPs was simulated in a 0.5 M sulfuric acid solution at 80°C. Figure 2 plots the polarization curves of specimens that were prepared with chemical conversion at 80 °C in a 0.5M H_2SO_4 solution for various periods. The curves reveal that the coatings underwent obvious passivation when the test passed through the OCP. The coatings exhibited pitting corrosion when the increase in the scanning electric potential dissolved the aluminum from the substrate, causing passivation in the substrate surface. The aluminum ions, dissolved from the aluminum substrate, reduced the activation energy of the reaction with the catalyst in fuel cell system. The passivation of the surfaces of the BBPs increased their interface resistance and reduced the efficacy of the fuel cells. Figure 2 also indicates that the coating that was converted for 1 min exhibited clear passivation, indicating that the oxide within the conversion coating was not enough to cover the substrate, so the corroding solution came into direct contact with the aluminum substrate. The passivation behavior that was caused by the aluminum ions that were dissolved from the aluminum substrate indicated that the conversion coatings exhibited some defects [26].

The coating that was converted for 5 min exhibited uniform corrosion behavior (Fig. 2) as the conversion coating was dense and uniform and completely covered the aluminum substrate without any cracks (Fig. 1(c)). The coating that was converted for 10 min also exhibited uniform corrosion

behavior (Fig. 2), but it was cracked (Fig. 1(d)), which reduced its corrosion resistance. The prolonged reaction resulted in the dissolution of the conversion coating into acid solution, forming defects in the coating. The I_{corr} values of the coatings that had been formed by conversion for 5 and 10 min at an ambient temperature of 80°C revealed a significant drop from 5.760×10^{-8} (5 min) to 7.983×10^{-5} (10 min). Therefore, the conversion coating that was formed at 5 min exhibited the best corrosion resistance (see Table 1).

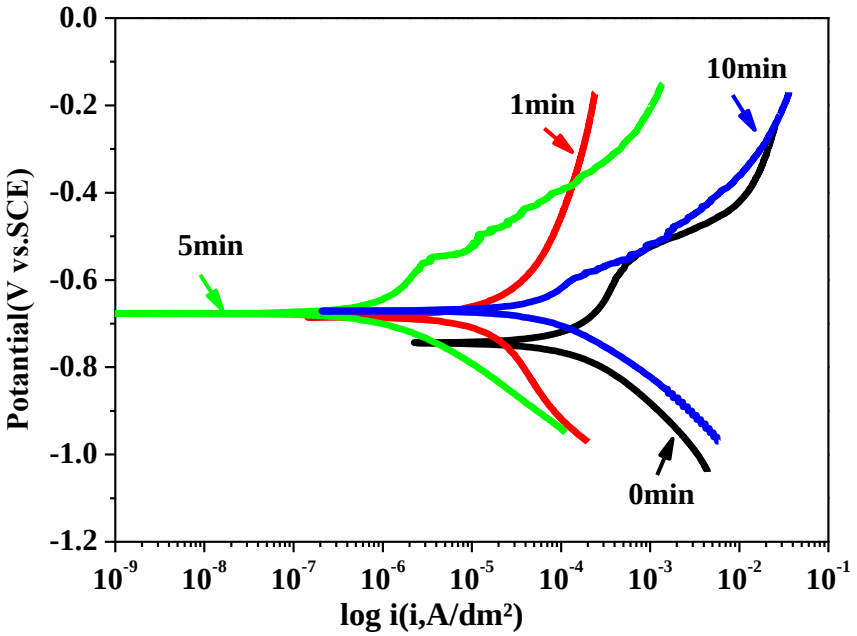

Figure 2. Polarization curves of aluminum alloy substrates following different chemical conversion treatment conditions at 80 °C in 0.5M H_2SO_4.

Table 1. Polarization tests conducted at 80 °C in a 0.5M H_2SO_4

Conversion Time	I(Corr.)(A/dm^2)	E(Corr.)(V)
Al alloy	8.345×10^{-5}	-0.711
1min	5.329×10^{-6}	-0.693
5min	5.760×10^{-8}	-0.672
10min	7.983×10^{-5}	-0.655

In general, the fuel cell systems must undergo potentiostatic measurements. The cathode of an operating fuel cell typically undergoes anodic corrosion. In this study, the simulated cathode potential was set to 0.6 V; the ambient temperature was set to 80 °C, and the operating time was 1 h. Figure 3 presents the current density recorded as a function of time for different conversion conditions. Gupta et al. [40] explained that the current density data characterised by numerous transients followed eventually by a large increase in current density to a relatively higher value indicating stable pitting corrosion. Figure 3(a) shows that the current density of the original aluminum alloy substrates increased with the operating time from 1.46×10^{-5} A/cm^2 to 3.46×10^{-5} A/cm^2 at 1 h of operation. The potentiostatic measurement reveals an unsteady state, and the highest current density during testing period was approximately 1.12×10^{-4} A/cm^2, indicating that the aluminum substrate exhibited pitting corrosion [41, 42], causing aluminum ions to dissolve from the substrate throughout the constant potential testing process.

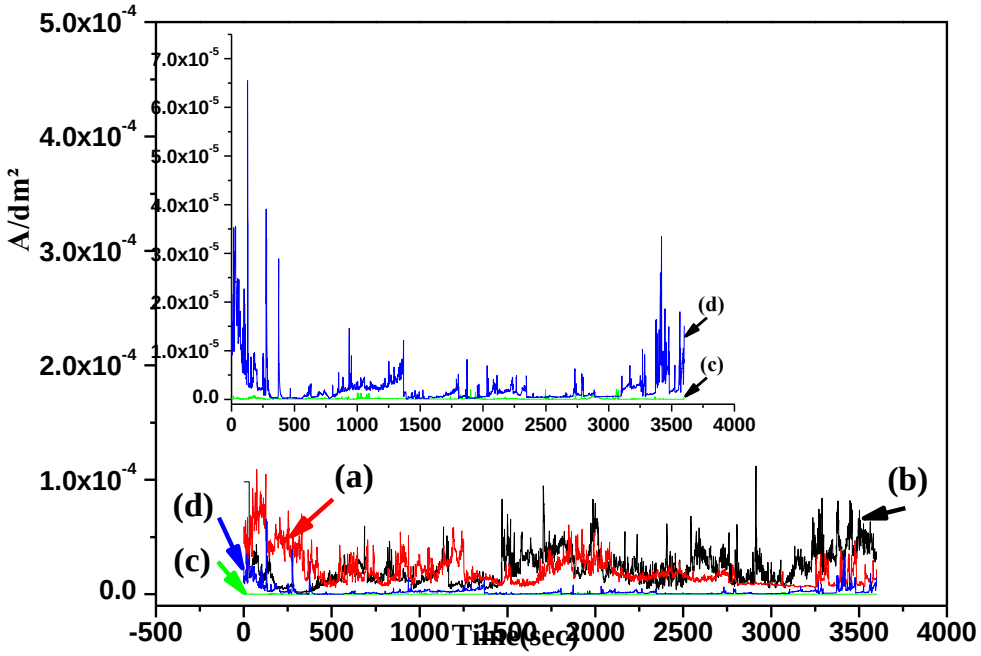

Figure 3. Current transients of aluminum alloy substrates following conversion treatment in H_2SO_4 solution at 80℃ applied 0.6 V (cathode environment): (a) no treatment, (b) 1min, (c) 5min and (d) 10min.

Figure 3(b) plots the current transients of the coating that was formed after 1 min of conversion: the same pitting corrosion condition was also evident, owing to the incompleteness of the coverage by the coating . Therefore, the aluminum ions easily dissolved from the substrate when 0.6 V was applied. Figure 3(c) shows the current transients of the coating that was formed by 5 min of conversion: the initial current density was about 1.45×10^{-7} A/cm^2; the final current density after 1 h of

potentiostatic measurement was approximately 1.47×10^{-7} A/cm^2, and the highest current density during the testing period was around 5.47×10^{-7} A/cm^2. Figure 3(c) also shows the relationship between the current density and the testing period is an almost straight line near the X axis, indicating that the conversion coating did undergo occur pitting corrosion but exhibited favorable or high corrosion resistance, protecting the aluminum substrate. Figure 3(d) shows the current transients of the coating formed after 10 min conversion process, it reveals an unstable condition, indicating that the coatings underwent pitting corrosion, and this indicates that the surface of the coating that was formed after 10 min of conversion exhibited defects including cracks.

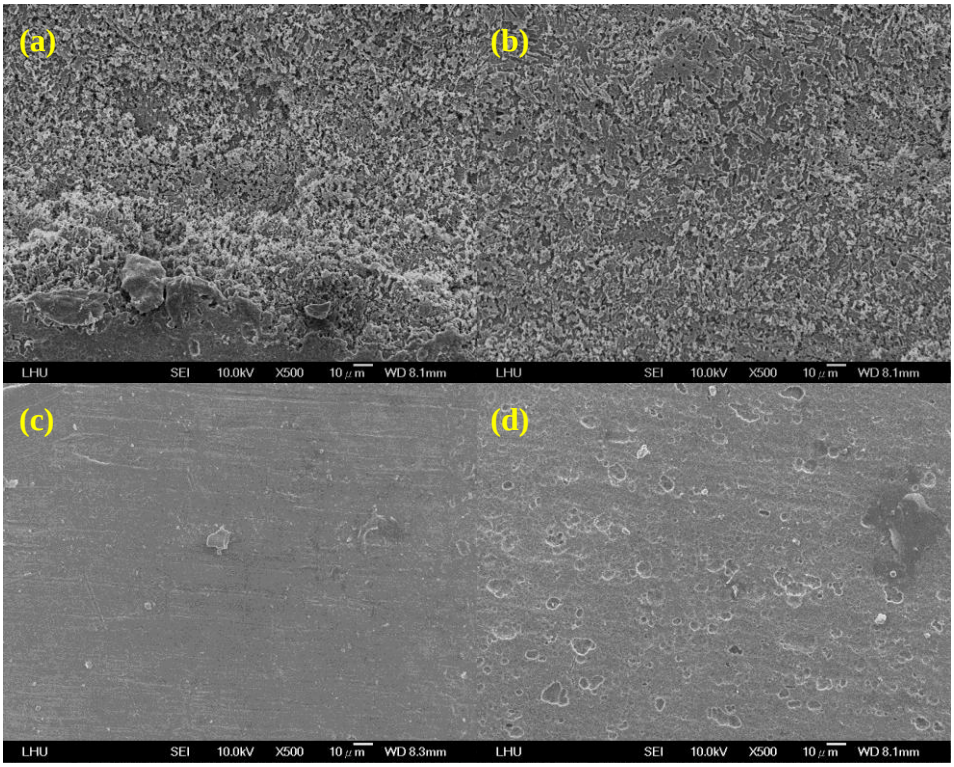

Figure 4. SEM micrographs of chemical conversion coatings in potentistatic polarization test: (a) no treatment, (b) 1min, (c) 5min and (d) 10min.

Figure 4 presents an SEM micrograph of chemical conversion coatings following the potentiostatic polarization test, the ICP analysis results is also listed at Table 2. Figure 4(a) shows large areas of pitting corrosion on the surface of the aluminum substrate under potentiostatic testing. The concentration of the aluminum ions that dissolved from the aluminum alloy substrate was approximately 216 ppm (Table 2). This result indicates that, in 0.5M H_2SO_4 solution, under an applied voltage of 0.6 V, the aluminum substrate could not resist pitting corrosion, so numerous aluminum ions dissolved from the aluminum alloy substrate. Figure 4(b) displays an SEM micrograph of chemical conversion coatings after 1 min of conversion, which is consistent with the polarization curves and reveals that these conversion coatings did not protect the aluminum alloy substrate. Figure 4(c) reveals the absence of any area of pitting corrosion in the conversion coatings after 5 min of

conversion, which had very dense microstructures. The potentiostatic polarization curves also show an absence of pitting corrosion on the surface of the conversion coatings after 5 min of conversion and the ICP analysis result shows that the concentration of aluminum ions that dissolved from the aluminum alloy substrate was only approximately 3.125 ppm (Table 2). Figure 4(d) reveals some areas of pitting corrosion of the conversion coatings after 10 min of conversion; their microstructures were not dense, and the concentration of aluminum ions that dissolved from the aluminum alloy substrate was approximately 47.326 ppm.

The above results reveal that 5 min of conversion was optimal for the conversion coatings, which then protected the substrate against 0.5M H_2SO_4 solution under an applied voltage of 0.6 V.

Table 2. ICP statistics from potentiostatic polarization test

Conversion Time	Al(ppm)	Cr(ppm)	Zr(ppm)
Al alloy	216.242	0	0
1min	228.162	0.012	0.342
5min	3.125	0.011	0.57
10min	47.326	0.570	1.881

The contact resistance of BBPs importantly affects the conductivity of fuel cells in which they are utilized. Figure 5 presents the contact resistance of aluminum alloy substrate formed following conversion. The figure shows that the aluminum alloy substrate exhibited excellent conductivity about 3.37×10^7/mΩ) and had such excellent properties as high strength and light weight; therefore, aluminum alloy after conversion treatment suited to use in BBPs in fuel cell systems than that of past studies [4,5]. Figure 5 also demonstrates that the substrates after conversion had a higher contact resistance than the initial substrates, when no pressure was applied, because the conversion coatings formed oxides. The contact area between the conversion coating and the carbon paper increased with the compaction force, reducing the contact resistance. The conversion coatings that underwent 5 min of conversion exhibited excellent contact resistance, which approached that of the aluminum alloy substrate when the compaction force increased to 150 N/cm^2, because oxides former within the conversion coatings with a greater total surface area than that of the aluminum alloy substrate. The contact area increased with the compaction force and the inter-space between BBPs and the carbon paper therefore decreased, reducing the contact resistance. The contact resistance value is about 8.6 m Ω cm^2 when the compaction force increased to 150 N/cm^2, and achieve the goal of U.S. DOE for bipolar plate application [43].

Figure 6 presents the cross-sectional TEM image of conversion coating after 5 min of conversion, and reveals that the coating was less thick and the microstructure was very dense. The thin conversion coatings approximately 100 nm thick retained the conductivity of the aluminum alloy

substrate, and their dense microstructures protected the aluminum alloy substrate and improved the corrosion resistance. It also reveals that the conversion coating after 5 min of conversion has excellent adhesion than that of forming by electro-less process [44], electroplating process [45] and pack chromization process [46]. Therefore, the thickness and microstructure of conversion coatings also affect contact resistance .

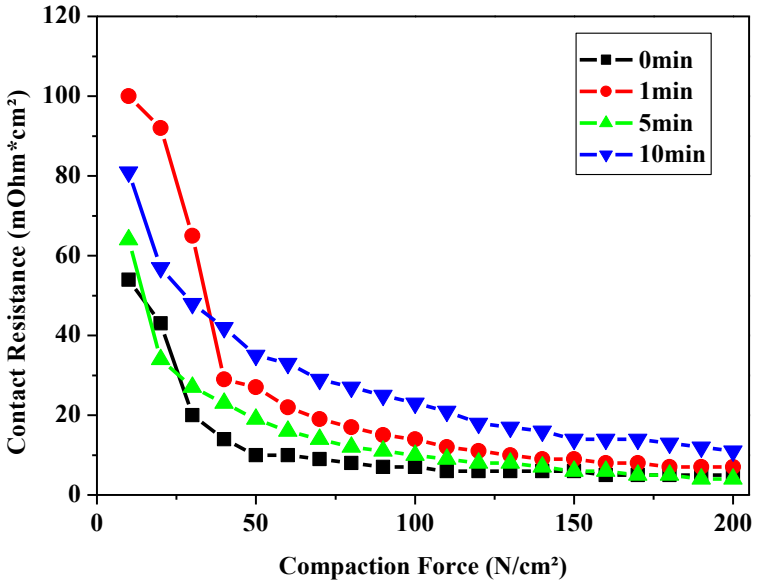

Figure 5. Variation of interfacial contact resistance with clamping pressure.

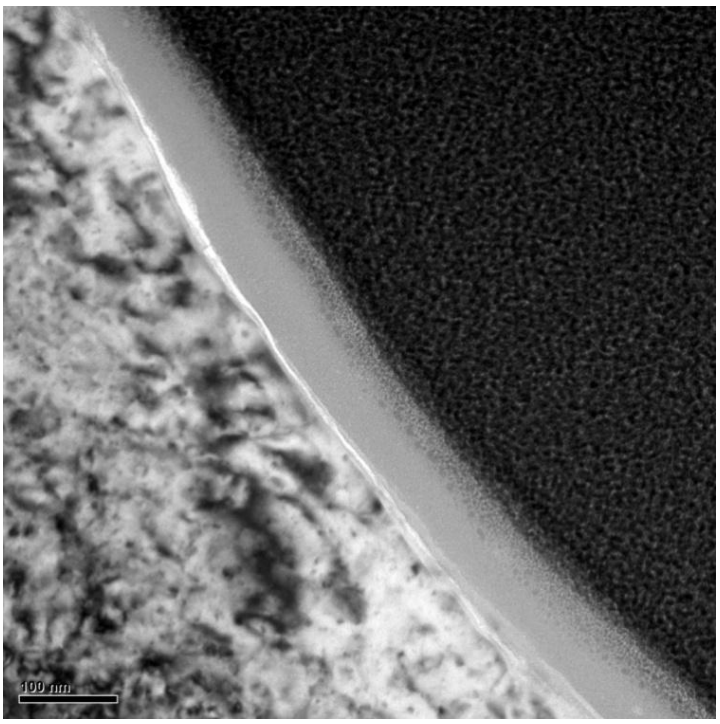

Figure 6. TEM cross-section micrographs of chemical conversion coatings with 5 min of conversion.

Figure 7 shows XPS depth profiles of conversion coatings after 5 min of conversion. The Al, O, Cr, Zr and Si contents are analyzed. Silicon was the alloy element in the aluminum alloy. Figure 7 presents the elemental analysis of the surfaces of the conversion coatings, which were found to include Al (approximately 9 at. %), O, Cr (about 5 at. %) and Zr (approximately 22 at. %), revealing that the conversion coatings included Al oxide, Cr oxide and Zr oxide.

Figure 8 plots the I-V curve that was obtained in single cell testing at 50 ^{0}C and 1 atm. The aluminum alloy substrate without a conversion coating had a high current density of about 1300 mA/cm^2 at the beginning of testing, dropping to 240 and 80 mA/cm^2 after working for 50 and 100 h, respectively, at an applied voltage of 0.5 V. The PEMFC performance using Zr-Cr oxide conversion coating in this study can rival with the past study that using a Ni-P coating on 5052 alloy substrate as BPPs [47].

This decrease is caused by the easy corrosion of the aluminum alloy in the working environment of the fuel cell, which serious reduces the efficacy of the cell. The result of single cell testing reveals that the aluminum alloy substrate after conversion passed a current density of approximately 1000 mA/cm^2 at the beginning testing, dropping to 500 mA/cm^2 after working for 100 h under an applied voltage at 0.5 V. These experimental results reveal that conversion coatings protect aluminum alloy substrates and improve the corrosion resistance of BBPs, favoring the efficacy of fuel cells in which they are used. Figure 9 plots the I-P curve obtained in single cell testing, which shows that the efficacy of the fuel cell after conversion was indeed better than that of the cell without conversion.

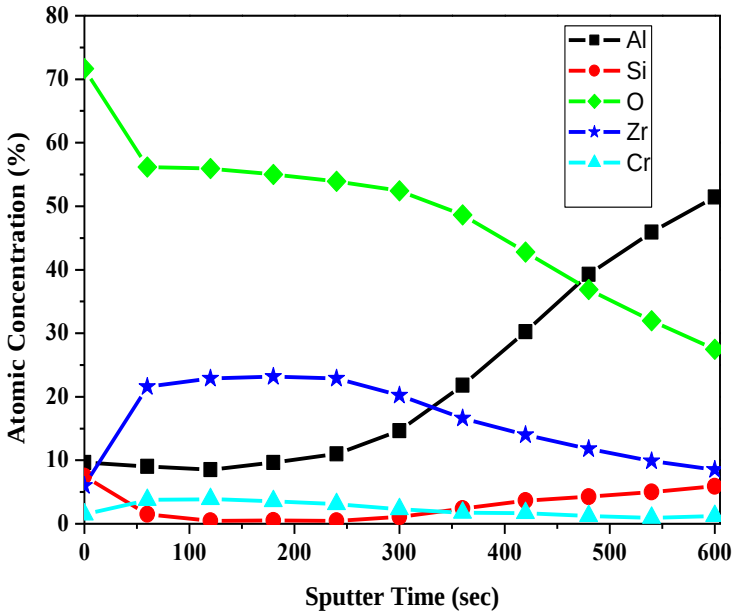

Figure 7. XPS depth profiles of Cr and Zr conversion coating.

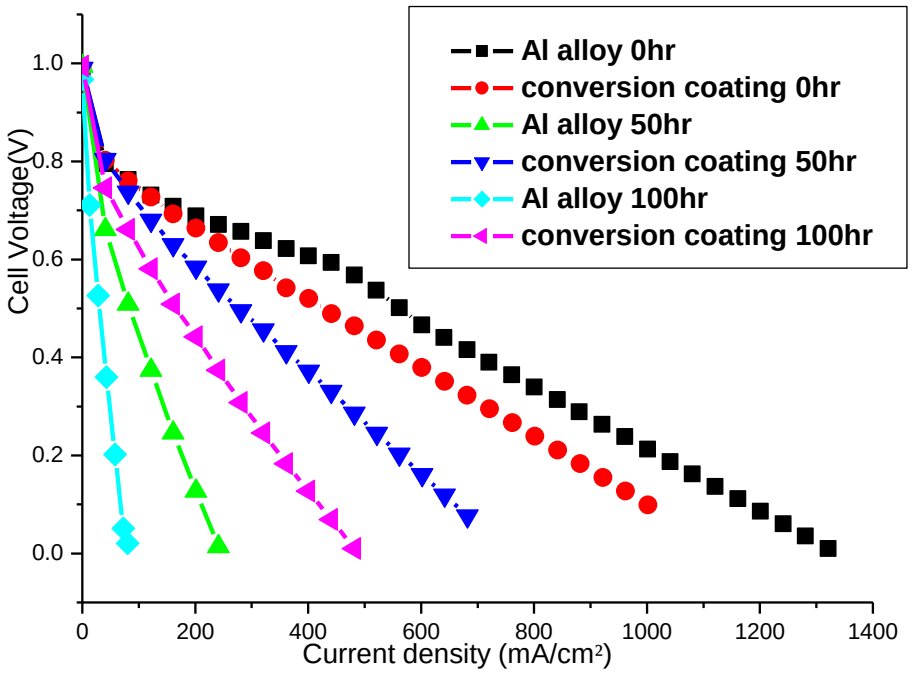

Figure 8. I–V curves of single cells assembled with the bare bipolar plates and bipolar plates with Al conversion coating; cell temperature = 50℃; QA =QC = 300cm^3 min^{-1}.

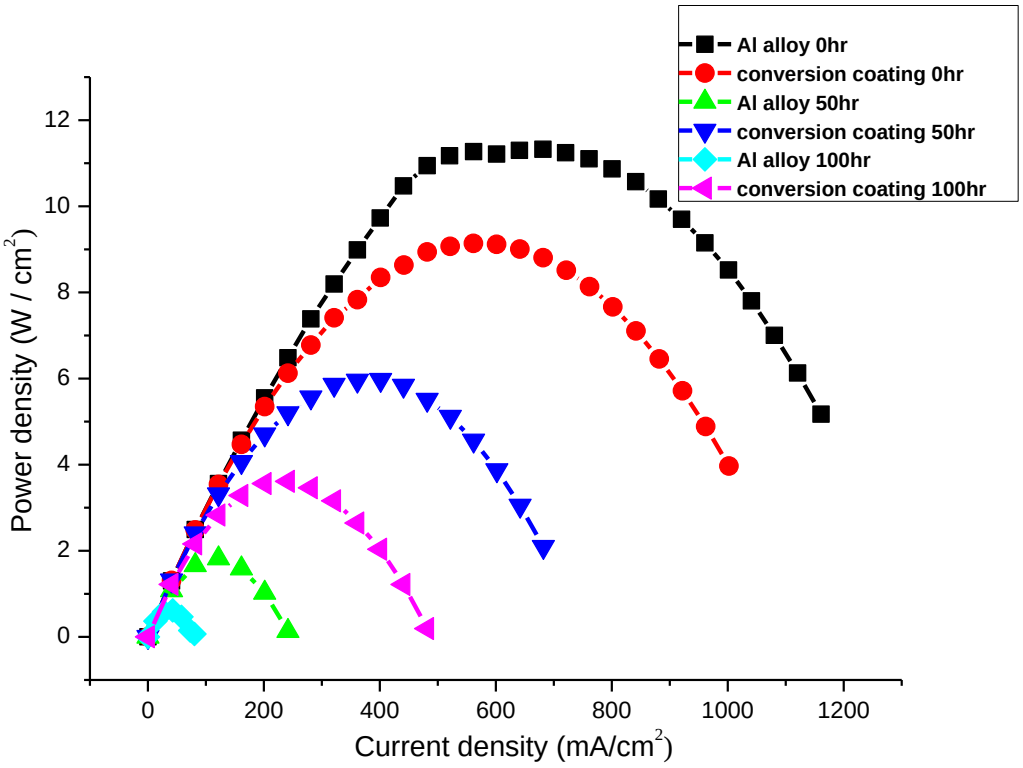

Figure 9. I–P curves of single cells assembled with bare bipolar plates and bipolar plates with Al conversion coating; cell temperature = 50 ℃; QA =QC = 300cm^3 min^{-1}.

4. CONCLUSIONS

1. The optimal I_{corr} of a crack-less conversion coating - 9.302×10^{-8}A/dm^2 at 25℃ and 5.760×10^{-8} A/dm^2 at 80℃ was obtained with 5 min of conversion .

2. The surfaces of conversion coatings after 5 min of conversion did not exhibit pitting corrosion, and they had very dense microstructures. The concentration of the aluminum ions that dissolved from the aluminum alloy substrate was only approximately 3.125 ppm.

3. The aluminum alloy substrate without conversion coatings had a high current density of approximately 1300 mA/cm^2 at the beginning of single cell testing, dropping to 80 mA/cm^2 after working for 100 h under an applied voltage of 0.5 V. Under the same operating conditions, the aluminum alloy substrate after 5 min of conversion had a current density of about 1000 mA/cm^2 at the beginning testing, dropping to 500 mA/cm^2 after working for 100 h. These results reveal that conversion coatings improve the corrosion resistance of substrates.

Reference

1. J. Ihonen, F. Jaouen, G. Lindberg and G. Sundholm, *Electrochim. Acta*, 46 (2001) 899.
2. Li X., "Principles of fuel cells" 1st ed. New York: Taylor: Francis Group; 2006.
3. E. Amani, R.M. Fetohi, H. Abdel, K.M. El-Khatib and E.R. Souaya, *International Journal of Hydrogen Energy*, 37 (2012) 7677.
4. C.Y. Bai, T.M. Wen, K.H. Hou and M.D. Ger, *Journal of Power Sources*, 195 (2010) 779.
5. C.Y. Bai, T.M. Wen, M.S. Huang, K.H. Hou, M.D. Ger and S.J. Lee, *Journal of Power Sources*, 195 (2010) 5686.
6. E.A. Cho, U.S. Jeon, S.A. Hong, I.H. Oh, S.G. Kang, *Journal of Power Sources*, 142 (2005) 77.
7. R. Tian, J. Sun, *Int. J. Hydrogen Energy*, 36 (2011) 6788.
8. R.Jennifer, J. Mawdsley, D. Carter, X. Wang, S. Niyogi, C. Q. Fan, R. Koc and G. Osterhoutd *Journal of Power Sources*, 231 (2013) 106.
9. T.M. Wen, K.H. Hou , C.Y. Bai , M.D. Ger , P.H. Chien and S.J. Lee, *Corros. Sci.*, 52 (2010) 3599.
10. I.E. Paulauskas, M.P. Brady, H.M. Meyer, R.A. Buchanan and L.R. Walker, *Corros. Sci.*, 48(2006) 3157.
11. S.J. Lee, C.H. Huang, J.J. Lai and Y.P. Chen, *Journal of Power Sources*, 131 (2004) 162.
12. Y. Fu, G.Q. Lin, M. Hou, B. Wu, Z. Shao and B. Yi, *International Journal of Hydrogen Energy*, 34 (2009) 405.
13. Y. Fu, M. Hou, G.Q. Lin, J.B. Hou, Z.G. Shao and B.L. Yi, *Journal of Power Sources*, 176 (2008) 282.
14. N.D.L. Heras, E.P.L. Roberts, R. Langton and D.R. Hodgson, *Energy Environmental Science*, 2 (2009) 206.
15. C. Davies, M. Barnett, *Journal of Organic Materials*, 56 (2004) 22.
16. L. Ma, S. Warthesen and D.A. Shores, *J. New Mater. Electrochem. Syst.*, 3 (2000) 221.
17. R. Hornung, G. Kappelt, *J. Power Sources*, 72 (1998) 20.
18. M.C. Li, C.L. Zeng, H.C. Lin and C.N. Cao, *Br. Corros. J.*, 36 (2001) 179.
19. M.C. Li, C.L. Zeng, S.Z. Luo , J.N. Shen, H.C. Lin and C.N. Cao, *Electrochim. Acta*, 48 (2003) 1735.
20. O.J. Murphy, A. Cisar and E. Clarke, *Electrochim. Acta* 43 (1998) 3829.
21. P.L. Hentall, J.B. Lakeman, G.O. Mepsted, P.L. Adcock and J.M. Moore, *Journal of Power Sources*, 80 (1999) 235.
22. D.R. Hodgson, B. May, P.L. Adcock and D.P. Davies, *Journal of Power Sources*, 96 (2001) 233.

23. L.E.M. Palomino, P.H. Suegama and I.V. Aoki, *Electrochim. Acta*, 52 (2007) 7496.
24. V. Guillaumin, G. Mankowski, *Corros. Sci.*, 41 (1998) 421.
25. Y. Liu, P. Skeldon, G. E. Thompson, H. Habazaki and K. Shimizu, *Corros. Sci.*, 46 (2004), 297.
26. W.K. Chen, C.Y. Bai, C.M. Liu, C.S. Lin and M.D. Ger, *Appl. Surf. Sci.*, 256 (2010) 4924.
27. W.K. Chen, J.L. Lee, C.Y. Bai, K.H. Hou and M.D. Ger, *Journal of the Taiwan Institute of Chemical Engineers* 43 (2012) 989.
28. J. Zhaoa, L. Xiaa, A. Sehgalb, D. Lub, R.L. McCreerya and G.S. Frankelb, *Surface and Coatings Technology* 140 (2001) 51.
29. A.S. Akhtar, K.C. Wong and K.A.R. Mitchell, *Surf. Coat. Technol.*, 253 (2006) 502.
30. Y. Yoon, R.G. Buchheit, *Electrochem. Solid State Lett.*, 11 (2005) 65.
31. L.Z. Long, C.Y. Zhou and L. Xiao, *Appl. Surf. Sci.*, 218 (2003) 123.
32. S. Natarajan, V. Ravikiran, *Surf. Eng.*, 22 (2006) 287.
33. A.A.O. Magalhaes, B. Tribollet, O.R. Mattos, I.C.P. Margarit and O.E. Barcia, *J. Electrochem. Soc.* 150 (2003) 16.
34. O. Lunder, J.C. Walmsley, P. Mack and K. Nisancioglu, *Corros. Sci.*, 47 (2005) 1604.
35. V. Palanivel, Y. Huang and W.J. Van Ooij, *Prog. Org. Coat*, 53 (2005) 153.
36. J. H. Lan, J. Kanicki, *Thin Solid Films*, 304 (1997) 123.
37. D.P. Davies, P.L. Adcock, M. Turpin, and S.J. Rowen, *Journal of Power Sources*, 86 (2000) 237.
38. S.J. Lee, C.H. Huang, J.J. Lai and Y.P. Chen, *Journal of Power Sources*, 131 (2004) 162.
39. H. Wang, M.A. Sweikar and J.A. Turner, *Journal of Power Sources*, 115 (2003) 243.
40. R.K. Gupta, B.R.W. Hinton and N. Birbilis, *Corros. Sci.*, 82 (2014) 197.
41. M.A. Amin, S.S.A. Ei-Rehim, E.E.F. Ei-Sherbini, S.R. Mahmoud and M.N. Abbas, *Electrochim Acta*, 54 (2009) 4288.
42. R.K. Gupta, N.L. Sukiman, M.K. Cavanaugh, B.R.W. Hinton, C.R. Hutchinson and N. Birbilis, *Electrochim Acta*, 66 (2012) 245
43. A. Mikrajuddin, F.G. Shi, H.K. Kim and K. Okuyama, *Mater. Sci.*, 2 (1999) 321.
44. S.Y. Tsai, C.Y. Bai, C.H. Lin, G.N. Shi, K.H. Hou, Y.M. Liu and M.D. Ger, *Journal of Power Sources*, 214 (2012) 51.
45. Amani E. Fetohi, R.M. Abdel Hameed, K.M. El-Khatib and Eglal R. Souaya, *International Journal of Hydrogen Energy*, 37 (2012) 7677.
46. C.Y. Bai, M.D. Ger and M.S. Wu, *International Journal of Hydrogen Energy*, 34 (2009) 6778.
47. C.H. Lin and S.Y. Tsai, *Applied Energy*, 100 (2012) 87.